

## Two-stage amplifier based on a double relaxation oscillation superconducting quantum interference device

M. Podt,<sup>a)</sup> M. J. van Duuren,<sup>b)</sup> A. W. Hamster, J. Flokstra,  
and H. Rogalla

*Low Temperature Division, Department of Applied Physics, University of Twente, P.O. Box 217,  
7500 AE Enschede, The Netherlands*

(Received 11 February 1999; accepted for publication 12 August 1999)

A low-noise single-chip two-stage superconducting quantum interference device (SQUID) system with a double relaxation oscillation SQUID as the second stage has been realized. The system was operated in a direct voltage readout mode, with a closed loop bandwidth up to 1 MHz. Operated at 4.2 K, the white flux noise measured in flux locked loop was  $1.3 \mu\Phi_0/\sqrt{\text{Hz}}$ , corresponding to an energy sensitivity of  $\epsilon \approx 27h$ . Owing to the large flux-to-voltage transfer of up to  $3.6 \text{ mV}/\Phi_0$ , the room-temperature preamplifier noise did not dominate the overall flux noise. © 1999 American Institute of Physics. [S0003-6951(99)01141-9]

A low  $T_c$  dc superconducting quantum interference device (SQUID)<sup>1</sup> is an extremely sensitive magnetic flux sensor with an intrinsic frequency response extending from dc to a few GHz. Any physical quantity that can be converted to magnetic flux, e.g., magnetic field, voltage, or mechanical displacement, can be measured very accurately.

A SQUID is commonly used as a flux-to-voltage converter. However, because of the small flux-to-voltage transfer of standard resistively shunted dc SQUIDs (typically  $\partial V/\partial\Phi = 100 \mu\text{V}/\Phi_0$ ), the typical flux noise of  $\sqrt{S_\Phi} = 1 \mu\Phi_0/\sqrt{\text{Hz}}$  corresponds to an output voltage noise of  $\sqrt{S_V} = 0.1 \text{ nV}/\sqrt{\text{Hz}}$ . This is about one order of magnitude lower than the input voltage noise of a low-noise room-temperature dc preamplifier, which leads to amplifier limitation of the system sensitivity. To solve this problem, ac flux modulation together with an impedance matching network is often used to amplify the SQUID output. Unfortunately, in this readout configuration the measurement bandwidth is limited by the modulation frequency, which is typically of the order of 100 kHz, although high bandwidth systems have been operated successfully.<sup>2</sup> Another disadvantage is possible crosstalk between adjacent channels of multichannel systems. Several new dc SQUID types with a larger flux-to-voltage transfer, so-called second generation dc SQUIDs, have been developed to allow a direct voltage readout mode without flux modulation. The flux-to-voltage transfer of these second generation dc SQUIDs, e.g., SQUIDs with additional positive feedback (APF),<sup>3</sup> double relaxation oscillation SQUIDs (DROSs),<sup>4,5</sup> and two-stage SQUID systems,<sup>6,7</sup> is of the order of  $1 \text{ mV}/\Phi_0$ .

This letter describes our development of a two-stage SQUID system with a DROS as the second stage, as shown schematically in Fig. 1. This second stage serves as a cryogenic low-noise preamplifier for the sensor SQUID, i.e., a standard low-noise resistively shunted nonhysteretic dc SQUID. Motivated by its large flux-to-voltage transfer and

low flux noise, a DROS with a reference junction<sup>8</sup> was chosen for the second stage instead of a conventional dc SQUID<sup>6</sup> or a series SQUID array.<sup>7</sup> The DROS had a gradiometric “figure-8” layout in order to minimize parasitic coupling between the sensor SQUID and the second stage. Figure 2(a) shows the schematic overview of the two-stage SQUID system we designed. The sensor SQUID is biased at a constant voltage by means of a small bias resistor  $R_{\text{bias}} \ll R_{\text{dyn}}$ , where  $R_{\text{dyn}}$  is the dynamic resistance of the sensor SQUID at the working point. The current  $I_1$  through the sensor SQUID is modulated by the applied signal flux  $\Phi_{\text{sig}}$  and is fed through the input coil of the DROS. Thus the current is converted to a magnetic flux  $\Phi_{2\text{nd}} = M_{\text{in},2}I_1$ , where  $M_{\text{in},2}$  is the mutual inductance between the DROS and its input coil. The second stage is biased at a constant current and the output signal of the two-stage SQUID system is the voltage across the DROS.

An important parameter in the design of a two-stage SQUID system is the flux gain  $G_\Phi = \partial\Phi_{2\text{nd}}/\partial\Phi_{\text{sig}}$ . The flux gain has to be sufficiently large, such that the amplified flux noise of the sensor SQUID is much larger than the flux noise added by the second stage and the readout electronics. If we want the flux noise of the second stage to contribute at most a fraction  $p$  to the total noise power, the flux gain should be at least

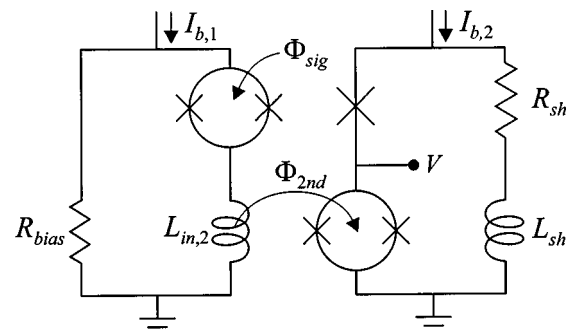


FIG. 1. Scheme of a two-stage SQUID system with a double relaxation oscillation SQUID as the second stage.

<sup>a)</sup>Electronic mail: m.podt@tn.utwente.nl

<sup>b)</sup>Present address: Philips Research Laboratories, Prof Holstlaan 4, 5656 AA Eindhoven, The Netherlands.

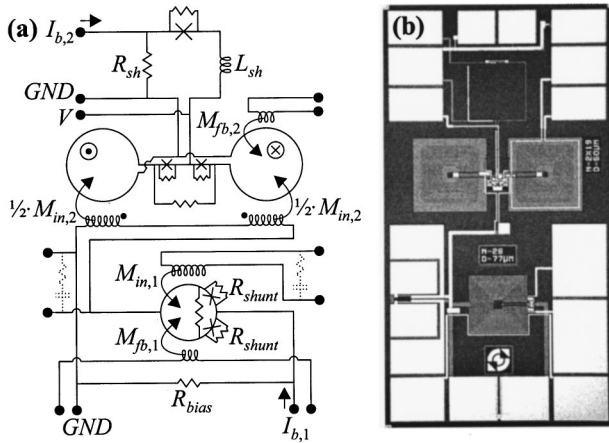


FIG. 2. (a) Scheme and (b) micrograph of the designed two-stage SQUID system with a gradiometric DROS as the second stage. The dashed  $R_{in}-C_{in}$  input coil shunts are not on-chip integrated.

$$G_{\Phi} \geq \sqrt{1/p-1} \cdot \sqrt{\frac{S_{\Phi,2}}{S_{\Phi,1}}} \Leftrightarrow G_{\Phi} \geq \sqrt{1/p-1} \cdot \sqrt{\frac{\epsilon_2}{\epsilon_1} \cdot \frac{L_{sq,2}}{L_{sq,1}}} \quad (1)$$

In this equation,  $\sqrt{S_{\Phi,i}}$  is the flux noise,  $\epsilon_i$  is the energy resolution, and  $L_{sq,i}$  is the SQUID inductance. The index  $i$  refers to the stage number. On the other hand, the available maximum flux gain can be estimated by

$$G_{\Phi} = M_{in,2} \cdot \frac{\partial I_1}{\partial \Phi_{sig}} \quad \text{with} \quad \frac{\partial I_1}{\partial \Phi_{sig}} = \frac{\partial I_1}{\partial I_{c,1}} \cdot \frac{\partial I_{c,1}}{\partial \Phi_{sig}} \quad (2)$$

In Eq. (2),  $I_{c,1}$  is the maximum critical current of the sensor SQUID. The factor  $\partial I_1 / \partial I_{c,1}$  can be approximated by  $R_{dyn} / (R_{dyn} + R_{bias})$ . By assuming sinusoidal behavior, the factor  $\partial I_{c,1} / \partial \Phi_{sig}$  can be calculated as

$$\left| \frac{\partial I_{c,1}}{\partial \Phi_{sig}} \right|_{\Phi_{sig} = 1/4\Phi_0} \approx \frac{4.4}{1 + \beta_{L,1}} \cdot \frac{I_{0,1}}{\Phi_0} \quad (3)$$

where  $I_{0,1}$  represents the critical current of one junction of the sensor SQUID and  $\beta_{L,1} = I_{c,1} L_{sq,1} / \Phi_0$  symbolizes the screening parameter of the sensor SQUID. The bandwidth of the two-stage SQUID system is limited by the cutoff frequency of the first stage, which is given by  $f_c = (R_{dyn} + R_{bias}) / (2\pi L_{in,2})$ , where  $L_{in,2}$  is the input coil inductance of the second stage.

We have designed and fabricated several two-stage SQUID systems, all of which had a sensor SQUID with an inductance of  $L_{sq,1} = 200$  pH and  $I_{c,1} = 11-12$   $\mu$ A. The  $4 \times 4$   $\mu\text{m}^2$  Nb/Al,  $\text{AlO}_x/\text{Al}/\text{Nb}$  Josephson junctions are defined by reactive ion etching in  $\text{SF}_6$ .<sup>9</sup> At 4.2 K, the white flux noise of the sensor SQUID was designed to be  $\sqrt{S_{\Phi, \text{theory}}} = 1.2$   $\mu\Phi_0 / \sqrt{\text{Hz}}$ ,<sup>1</sup> corresponding to a theoretical energy resolution of  $\epsilon = S_{\Phi, \text{theory}} / 2L_{sq,1} = 23h$ . The sensor SQUID was biased at a constant voltage by means of a bias resistor with a resistance of  $R_{bias} = 0.5$   $\Omega$ . A 28-turns input coil was deposited on top of the sensor SQUID washer. The mutual inductance between this input coil and the sensor SQUID was measured to be  $M_{in,1} = 4.2$  nH.

Two different gradiometric DROSs, labeled A and B, were used as the second stage. DROS A had a SQUID inductance of  $L_{sq,2} = 550$  pH and a  $2 \times 25$ -turns input coil with inductance  $L_{in,2} = 150$  nH. The mutual inductance between

TABLE I. Electrical parameters of the two-stage SQUID systems.

Electrical parameter	Sensor SQUID	DROS A	DROS B
$L_{sq}$ (pH)	200 <sup>b</sup>	550 <sup>b</sup>	490 <sup>b</sup>
$I_{c,1} = 2I_0$ ( $\mu$ A)	11–12 <sup>b</sup>	4–5 <sup>b</sup>	4–5 <sup>b</sup>
$\beta_L = 2I_0 L_{sq} / \Phi_0$	1.1	1.2	1.1
$R_{shunt}$ ( $\Omega$ )	7 <sup>b</sup>	47 <sup>a</sup>	47 <sup>a</sup>
$C_j$ (pF)	0.5 <sup>a</sup>	0.2 <sup>a</sup>	0.2 <sup>a</sup>
$\beta_c = 2\pi I_0 R_{shunt}^2 C_j / \Phi_0$	0.4	3	3
$L_{in}$ (nH)	95 <sup>a</sup>	150 <sup>b</sup>	87 <sup>a</sup>
$M_{in}$ (nH)	4.2 <sup>b</sup>	6.7 <sup>b</sup>	4.7 <sup>b</sup>
$\sqrt{S_{\Phi}}$ ( $\mu\Phi_0 / \sqrt{\text{Hz}}$ )	1.2 <sup>a,b</sup>	6 <sup>b</sup>	6 <sup>b</sup>
$\partial V / \partial \Phi$ (mV/ $\Phi_0$ )	0.1 <sup>b</sup>	0.4 <sup>b</sup>	0.4 <sup>b</sup>

<sup>a</sup>Design/calculated value.

<sup>b</sup>Experimental value.

the input coil and the DROS inductance is  $M_{in,2} = 6.7$  nH. The measured white flux noise of the DROS A in flux locked loop is typically  $6$   $\mu\Phi_0 / \sqrt{\text{Hz}}$ .<sup>8</sup> Consequently, if we require that  $p = 5\%$ , the flux gain should be at least 22 [from Eq. (1)]. According to Eq. (2), the maximum available flux gain is  $G_{\Phi} = 36$ . The theoretical cutoff frequency of the first stage is  $f_c = 5$  MHz. DROS B had a SQUID inductance of 490 pH, a  $2 \times 19$ -turns input coil with  $L_{in,2} = 87$  nH and a mutual inductance between the input coil and the DROS of  $M_{in,2} = 4.7$  nH. The maximum available flux gain is  $G_{\Phi} = 26$  and the maximum cutoff frequency is  $f_c = 9$  MHz. For both DROSs, the available flux gain is larger than the required flux gain of 22. Figure 2(b) shows a micrograph of one of the integrated two-stage SQUID systems with DROS B as second stage. The actual chip size is  $2.2 \times 4$   $\text{mm}^2$ . The most important parameters of the two-stage SQUID systems are summarized in Table I.

The two-stage SQUID systems were characterized by using home-made flux locked loop (FLL) electronics based on direct voltage readout.<sup>8,10</sup> In closed loop, a  $-3$  dB bandwidth up to 1 MHz was achieved. By improving the room-temperature electronics, even higher bandwidths might be possible.

Figure 3 shows the measured  $V - \Phi_{sig}$  characteristics of one of the two-stage SQUID systems with DROS A as second stage. Multiple oscillation periods in the second stage occur for only one modulation period in the first stage, caused by the flux gain. The readout DROS was biased at a current  $I_{b,2} = 54$   $\mu$ A, the bias current of the first stage, and thus the bias voltage of the sensor SQUID, was varied. The maximum voltage modulation was about 40  $\mu$ V and the maximum flux-to-voltage transfer was  $\sim 3.6$  mV/ $\Phi_0$ .

The actual flux gain depends on the bias voltage of the sensor SQUID. The higher the bias voltage, the lower the modulation depth in the current through the sensor SQUID and the lower the flux gain. At low bias voltages, the designed maximum flux gain could be achieved.

Moreover, the flux gain depends on the applied flux. The flux gain is maximum at the working point,  $\Phi_{sig} = (1/4 + n/2)\Phi_0$ . At that point, the largest amount of wide band flux noise is coupled from the sensor SQUID to the second stage, which causes the voltage modulation depth of the DROS to decrease somewhat. This effect was the largest for the wide band two-stage SQUID systems with DROS B as the second stage. Consequently the flux-to-voltage transfer of these sensors was only  $\sim 1.7$  mV/ $\Phi_0$ .

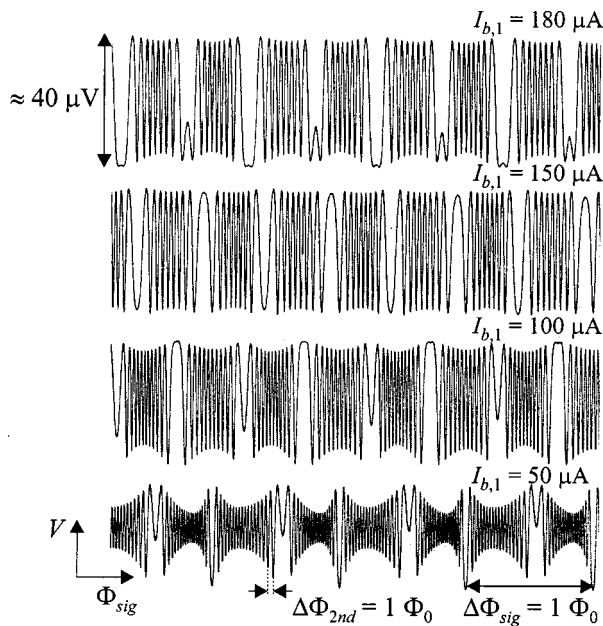


FIG. 3. Experimental  $V-\Phi_{\text{sig}}$  characteristics of the two-stage SQUID system with DROS A as the second stage for different bias currents of the first stage, indicated at the right. The signal flux was applied via the feedback coil of the first stage. The bias current of the second stage was fixed at  $I_{b,2} \approx 54 \mu\text{A}$ .

The noise spectrum of the two-stage SQUID system with DROS A measured in FLL at 4.2 K is shown in Fig. 4. By applying an offset flux to the sensor SQUID and the second stage, the system was locked at  $\Phi_{\text{sig}} = (1/4 + n/2)\Phi_0$ , the point of maximum flux gain. The bias current of the first stage was  $I_{b,1} = 80 \mu\text{A}$  and the second stage was biased at  $I_{b,2} = 54 \mu\text{A}$ . The total white flux noise is  $\sqrt{S_{\Phi}} \approx 1.3 \mu\Phi_0/\sqrt{\text{Hz}}$ , corresponding to an energy resolution of  $\epsilon = S_{\Phi}/2L_{\text{sq},1} \approx 27h$ . This corresponds well to the theoretical white flux noise of the sensor SQUID, which means that the system sensitivity of the two-stage SQUID systems is indeed determined by the sensor SQUID and not by the second stage or the readout electronics. The total white flux noise of the two-stage SQUID system with DROS B was somewhat higher,  $\sqrt{S_{\Phi}} \approx 2.1 \mu\Phi_0/\sqrt{\text{Hz}}$ . In that case, the noise contribution of the readout electronics was larger because of the smaller flux-to-voltage transfer, due to the smaller flux gain.

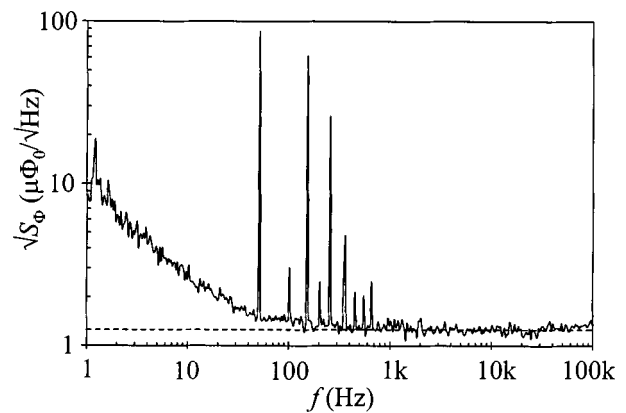


FIG. 4. Flux noise spectrum of the two-stage SQUID with DROS A as the second stage, measured at 4.2 K.

In conclusion, we designed, fabricated, and characterized two-stage SQUID systems with a DROS as the second stage. The large flux-to-voltage transfer of the DROS together with the low flux noise makes the DROS particularly suitable as the second stage. The large flux-to-voltage transfer of the two-stage SQUID systems enabled a direct voltage readout mode without ac flux modulation and without amplifier limitation of the system sensitivity. Consequently, the total measured white flux noise was very close to the theoretical flux noise of the sensor SQUID.

- <sup>1</sup>C. D. Tesche and J. Clarke, *J. Low Temp. Phys.* **29**, 301 (1977).
- <sup>2</sup>R. H. Koch, J. R. Rozen, P. Wöltgens, T. Picunco, W. J. Goss, F. Gambrel, D. Lathrop, R. Wiegert, and D. Overway, *Rev. Sci. Instrum.* **67**, 2968 (1996).
- <sup>3</sup>D. Drung, *Appl. Phys. Lett.* **67**, 1474 (1995).
- <sup>4</sup>D. J. Adelerhof, H. Nijstad, J. Flokstra, and H. Rogalla, *J. Appl. Phys.* **76**, 3875 (1994).
- <sup>5</sup>D. J. Adelerhof, J. Kawai, G. Uehara, and H. Kado, *Appl. Phys. Lett.* **65**, 2606 (1994).
- <sup>6</sup>D. E. Kirichenko, A. B. Pavolotskij, O. V. Snigirev, R. Mezzena, S. Vitale, A. V. Beljaev, and Y. V. Maslennikov, *IEEE Trans. Appl. Supercond.* **7**, 1045 (1997).
- <sup>7</sup>R. P. Welty and J. M. Martinis, *IEEE Trans. Appl. Supercond.* **3**, 2605 (1993).
- <sup>8</sup>M. J. van Duuren, G. C. S. Brons, D. J. Adelerhof, J. Flokstra, and H. Rogalla, *J. Appl. Phys.* **82**, 3598 (1997).
- <sup>9</sup>D. J. Adelerhof, M. E. Bijlsma, P. B. M. Fransen, T. Weiman, J. Flokstra, and H. Rogalla, *Physica C* **209**, 477 (1993).
- <sup>10</sup>A. W. Hamster, M. J. van Duuren, G. C. S. Brons, J. Flokstra, and H. Rogalla, *IEEE Trans. Appl. Supercond.* **9**, 2915 (1999).